

The Vacuolar Import and Degradation Pathway Merges with the Endocytic Pathway to Deliver Fructose-1,6-bisphosphatase to the Vacuole for Degradation*

Received for publication, December 5, 2007, and in revised form, July 25, 2008. Published, JBC Papers in Press, July 25, 2008, DOI 10.1074/jbc.M709922200

C. Randell Brown, Allison B. Wolfe, Dongying Cui, and Hui-Ling Chiang¹

From the Department of Cellular and Molecular Physiology, Penn State University College of Medicine, Hershey, Pennsylvania 17033

The gluconeogenic enzyme fructose-1,6-bisphosphatase (FBPase) is degraded in the vacuole when glucose is added to glucose-starved cells. Before it is delivered to the vacuole, however, FBPase is imported into intermediate carriers called Vid (vacuole import and degradation) vesicles. Here, using biochemical and genetic approaches, we identified a requirement for SEC28 in FBPase degradation. SEC28 encodes the ϵ -COP subunit of COPI (coat protein complex I) coatomer proteins. When SEC28 and other coatomer genes were mutated, FBPase degradation was defective and FBPase association with Vid vesicles was impaired. Coatomer proteins were identified as components of Vid vesicles, and they formed a protein complex with a Vid vesicle-specific protein, Vid24p. Furthermore, Vid24p association with Vid vesicles was impaired when coatomer genes were mutated. Kinetic studies indicated that Sec28p traffics to multiple locations. Sec28p was in Vid vesicles, endocytic compartments, and the vacuolar membrane in various mutants that block the FBPase degradation pathway. Sec28p was also found in vesicles adjacent to the vacuolar membrane in the *ret2-1* coatomer mutant. We propose that Sec28p resides in Vid vesicles, and these vesicles converge with the endocytic pathway. After fusion, Sec28p is distributed on the vacuolar membrane, where it concentrates on vesicles that pinch off from this organelle. FBPase also utilizes the endocytic pathway for transport to the vacuole, as demonstrated by its presence in endocytic compartments in the $\Delta vph1$ mutant. Taken together, our results indicate a strong connection between the Vid trafficking pathway and the endocytic pathway.

Transport of proteins and lipids between organelles is an important function of all eukaryotic cells. In many cases, vesicles facilitate the transport of cargo proteins or lipids from donor membranes to acceptor membranes (1–10). The most thoroughly studied transporters are coat protein complex I (COPI),² COPII, and clathrin-coated vesicles. COPI vesicles

mediate the retrograde transport from the Golgi to the ER as well as intra-Golgi transport, whereas COPII-coated vesicles conduct anterograde transport from the ER to Golgi. The clathrin-coated vesicles regulate trafficking from the plasma membrane to early endosomes and from the Golgi to endosomes (1–10).

Characterization of COPI vesicles has revealed the presence of a protein complex called “coatomer.” Coatomer is a cytosolic protein complex comprised of seven subunits, α -COP (160 kDa), β -COP (110 kDa), β' -COP (102 kDa), γ -COP (98 kDa), δ -COP (61 kDa), ϵ -COP (35 kDa), and ζ -COP (20 kDa) (11–13). The COPI coats have been detected on the Golgi complex and on the ER (14, 15). Coatomer subunits have also been found in endocytic compartments in mammalian cells and yeast (16–21). Furthermore, they play an important role in endocytic trafficking in both mammalian cells (16–20), and in yeast (21). In addition to coatomer, the GTPase ARF (ADP-ribosylation factor) associates with COPI vesicles in its GTP bound form. This protein is needed for the formation of COPI vesicles (22).

Several vesicle-mediated protein trafficking pathways have been identified in *Saccharomyces cerevisiae* (23–26). For example, a specialized autophagy pathway has been studied in our laboratory. This pathway utilizes a novel type of vesicle called Vid (vacuole import and degradation) vesicles, which transport cargo such as fructose-1,6-bisphosphatase (FBPase). FBPase is a key regulatory enzyme in gluconeogenesis. This enzyme is induced when yeast cells are grown under glucose starvation conditions. However, when glucose-starved cells are shifted to fresh glucose, FBPase is rapidly inactivated and then degraded (27–30). The glucose-induced degradation of FBPase has been reported to occur both in the proteasome (31–33) and in the vacuole (27–30, 34–36). Interestingly, the length of glucose starvation was found to account for this difference (35). For example, when cells were starved for a short period of time and then shifted to glucose, FBPase was degraded in the proteasome. However, when glucose was added to cells that have been starved for longer periods of time, FBPase was degraded in the vacuole (35). Malate dehydrogenase (MDH2) is another gluconeogenic enzyme that shares degradation characteristics with FBPase. Short-term starvation leads to proteasome-dependent degradation of MDH2, whereas long-term starvation leads to vacuolar degradation of this protein (35).

* This work was supported, in whole or in part, by National Institutes of Health Grant RO1GM59480 (to H.-L. C.). The costs of publication of this article were defrayed in part by the payment of page charges. This article must therefore be hereby marked “advertisement” in accordance with 18 U.S.C. Section 1734 solely to indicate this fact.

¹ To whom correspondence should be addressed: 500 University Dr., Hershey, PA 17033. Tel.: 717-531-0860; Fax: 717-531-7667; E-mail: hlchiang@psu.edu.

² The abbreviations used are: COPI, coat protein complex I; ER, endoplasmic reticulum; FBPase, fructose-1,6-bisphosphatase; ARF, ADP-ribosylation factor; HA, hemagglutinin; DSP, dithiobis(succinimidyl propionate); GFP,

green fluorescent protein; MALDI, matrix-assisted laser desorption/ionization; Vid, vacuole import and degradation.

TABLE 1

Strains used in this study

Deletion strains derived from BY4742 were from Euroscarf.

Strain	Genotype
HLY635	<i>MATα ura3-52 LEU2 trp1Δ63 his3Δ200 GAL2</i>
BY4742	<i>MATα his3Δ1 leu2Δ0 lys2Δ0 ura3Δ0</i>
Δ <i>sec28</i>	<i>MATα his3Δ1 leu2Δ0 lys2Δ0 ura3Δ0 sec28::kanMX4</i>
HLY1080	<i>MATα leu2Δ0 lys2Δ0 ura3Δ0 FBPaase-GFP::HIS3</i>
HLY1385	<i>MATα leu2Δ0 lys2Δ0 ura3Δ0 sec28::kanMX4 FBPaase-GFP::HIS3</i>
HLY 2119	<i>MATα his3Δ1 leu2Δ0 lys2Δ0 ura3Δ0 vam3::kanMX4 FBPaase-GFP::HIS3</i>
HLY225	<i>MATα his3-Δ200 ura3-52 leu2,3-112 lys2-801 vid24::TRP1</i>
Δ <i>vam3</i>	<i>MATα his3Δ1 leu2Δ0 lys2Δ0 ura3Δ0 vam3::kanMX4</i>
HLY1023	<i>MATα leu2Δ0 lys2Δ0 ura3Δ0 vam3::kanMX4 VID24-HA::HIS3</i>
HLY1816	<i>MATα leu2Δ0 lys2Δ0 ura3Δ0 sec2-1 Vid24-HA::HIS3</i>
RSY1010	<i>MATα ura3 leu2 sec21-1</i>
RH3517	<i>MATα ura3 his3 leu2 lys2 suc2Δ9 ret3-1 mycSTE2EMP47tail::URA3</i>
RH3521	<i>MATα sec27-1 his4 ura3 leu2 bar1 mycSTE2EMP47tail::URA3</i>
RH3516	<i>MATα his3 ura3 leu2 lys2 suc2Δ9 ret2-1 mycSTE2EMP47tail::URA3</i>
YW05	<i>MATα lys1 leu2 ura3 trp1 ubc1::HIS3</i>
Δ <i>ise1</i>	<i>MATα his3Δ1 leu2Δ0 lys2Δ0 ura3Δ0 ise1::kanMX4</i>
Δ <i>arf1</i>	<i>MATα his3Δ1 leu2Δ0 lys2Δ0 ura3Δ0 arf1::kanMX4</i>
HLY228	<i>MATα leu2Δ0 lys2Δ0 ura3Δ0 VID24-HA::HIS3</i>
HLY1386	<i>MATα leu2Δ0 lys2Δ0 ura3Δ0 sec28::kanMX4 VID24-HA::HIS3</i>
HYL1817	<i>MATα leu2 ura3 ret2-1 Vid24-HA::HIS3</i>
HLY1816	<i>MATα leu2 ura3 sec21-1 Vid24-HA::HIS3</i>
HLY1422	<i>MATα ura3 leu2 lys1 Sec28p-GFP::HIS3</i>
Δ <i>ypt7</i>	<i>MATα his3Δ1 leu2Δ0 lys2Δ0 ura3Δ0 ypt7::kanMX4</i>
Δ <i>ubc1</i>	<i>MATα his3Δ1 leu2Δ0 lys2Δ0 ura3Δ0 ubc1::kanMX4</i>
Δ <i>vph1</i>	<i>MATα his3Δ1 leu2Δ0 lys2Δ0 ura3Δ0 vph1::kanMX4</i>
HLY1412	<i>MATα his3Δ1 leu2Δ0 lys2Δ0 ura3Δ0 vam3::kanMX4 Sec28p-GFP::HIS3</i>
HLY1463	<i>MATα his3Δ1 leu2Δ0 lys2Δ0 ura3Δ0 ubc1::kanMX4 Sec28p-GFP::HIS3</i>
HLY1793	<i>MATα his3 ura3 leu2 lys2 suc2Δ9 ret2-1 mycSTE2EMP47tail::URA3 Sec28p-GFP::HIS3</i>
HLY2113	<i>MATα his3Δ1 leu2Δ0 lys2Δ0 ura3Δ0 vph1::kanMX4 Sec28p-GFP::HIS3</i>
HLY1747	<i>MATα leu2Δ0 lys2Δ0 ura3Δ0 vph1::kanMX4 FBPaase-GFP::HIS3</i>
Δ <i>pep4</i>	<i>MATα leu2Δ0 lys2Δ0 ura3Δ0 pep4::kanMX4</i>
W303	<i>MATα ura3 leu2 his3 trp1 lys2 ade2</i>

FBPase is transported to the vacuole via Vid vesicles (36). At present, the origin of these vesicles has not been established, although we have partially characterized these structures. As such, we have determined that FBPase import into Vid vesicles requires the heat shock protein Ssa2p (37), Vid22p (38), and cyclophilin A (39). Once they are loaded, Vid vesicles are transported to the vacuole through a process that is dependent on the presence of Vid24p, Ypt7p, SNARE proteins, and V-ATPase (40, 41). As stated above, the origin of Vid vesicles remains unknown. This is largely due to the lack of specific Vid vesicle markers. Vid24p remains the only known marker for these structures to date. Further complicating these studies, Vid24p is present at very low levels prior to a glucose shift. Synthesis of Vid24p does increase following a glucose shift for 20 min, at which point it localizes to Vid vesicles as a peripheral protein (28).

In our previous studies, multiple FBPase containing organelles have been observed to accumulate in *vid* mutants (30), suggesting that organelles other than Vid vesicles may also be involved in the delivery of FBPase to the vacuole (30). In an attempt to identify additional Vid vesicle marker proteins and track the Vid vesicle trafficking pathway, purified vesicle fractions were subjected to MALDI analysis. Via this method, we identified COPI coatomer proteins including Sec28p, Sec21p, and Ret1p as components of purified Vid vesicles. *SEC28*, which encodes the ϵ -COP component of coatomers (42, 43), was also identified independently via the screening of a deletion library using a previously established colony blot protocol (30).

Here, we show that *SEC28* and coatomer genes play a role in the FBPase degradation process. Δ *sec28* and coatomer mutants exhibited defective FBPase degradation, whereas FBPase asso-

ciation with Vid vesicles was also impaired in these mutant strains. Moreover, coatomer subunits were found in Vid vesicle containing fractions, where they formed a protein complex with Vid24p. Sec28p was also found in Vid vesicles, endosomes, and vacuole membranes in various mutants that block the FBPase degradation pathway. We propose that Sec28p resides on Vid vesicles, and these vesicles later merge with the endocytic pathway. This idea was further confirmed by a study of FBPase distribution in the Δ *vph1* strain. FBPase was initially in the cytosol but moved to endocytic compartments at later time points. This suggests that FBPase enters the endocytic pathway following a glucose shift. Taken together, our results establish a strong connection between the endocytic pathway and the vacuole import and degradation pathway that delivers cytosolic FBPase to the vacuole for degradation.

EXPERIMENTAL PROCEDURES

Yeast Strains, Antibodies, and Primers—*S. cerevisiae* strains used in this study are listed in Table 1. The deletion strains derived from BY4742 were from Euroscarf (Euroscarf, Germany). The coatomer mutants (*ret1-1*, *ret1-3*, *sec21-1*, and *sec27-1*) and anti-Sec28p sera were gifts from Dr. Rainer Duden (University of Cambridge, UK). The coatomer mutants (*ret2-1*, *ret3-1*, *sec21-1*, and *sec27-1*) were gifts from Dr. Howard Riezman (University of Geneva, Switzerland). Anti-coatomer sera were obtained from Dr. R. Schekman (University of California, Berkeley, CA). The rhodamine goat anti-mouse and fluorescein goat anti-rabbit antisera were purchased from Covance. Mouse monoclonal anti-HA was purchased from Roche. The enhanced chemiluminescence kit was purchased from

The Vid Degradation Pathway Merges with the Endocytic Pathway

TABLE 2

Primers used in this study

Primers	
FBPase-GFP	Forward
	Reverse
Vid24p-HA	Forward
	Reverse
Sec28p-GFP	Forward
	Reverse

PerkinElmer Life Sciences. Primers used in this study are listed in Table 2.

FBPase Colony Blot Assay—The colony blot assay was performed as described (30). A yeast deletion library was plated on YPKG plates for 5–7 days at 22 °C, after which mutant strains were replica plated onto nitrocellulose membranes. Nitrocellulose membranes were incubated with affinity purified anti-FBPase antibodies at 1:1000 dilution, washed, and incubated with alkaline phosphatase-conjugated goat anti-rabbit antibodies at 1:5000 dilution. FBPase degradation-deficient mutants were identified as dark purple colonies. *SEC28* was identified using this method.

Differential Centrifugation, Sucrose Density Gradients, S-1000 Chromatography, Immunoprecipitation, and Cross-linking—Differential centrifugation and sucrose density gradients were conducted as described previously (37, 40). S-1000 chromatography was performed as described (30). Yeast cells expressing Vid24p-HA were grown in YPKG (50 ml) for 2 days and shifted to YPD for 30 min. Cells were harvested and cell lysates were subjected to differential centrifugation. Vid vesicle-enriched pellet fractions were further fractionated on sucrose density gradients. Fractions were collected and proteins from each fraction were blotted with anti-HA, anti-Sec28p, or anti-coatomer antibodies. For immunoprecipitation experiments, Vid vesicle-enriched fractions from the sucrose gradients were pooled, followed by 2% Triton X-100 solubilization. After centrifugation at 13,000 × *g* for 20 min at 4 °C, the supernatant was then incubated with 2 μl of anti-HA antibodies, followed by 100 μl of a 50% slurry of protein G beads (Amersham Biosciences). Beads were then washed three times and the bound and unbound fractions were detected by Western blotting with anti-HA, anti-Sec28p, anti-FBPase, and anti-coatomer antibodies. Chemical cross-linking experiments were performed on selected fractions as described previously (44) with minor modifications. Briefly, DSP was added to 100 μl of the sucrose gradient fraction to a final concentration of 1 mg/ml. Samples were incubated on ice for 45 min and the reaction was quenched via the addition of 50 μl of 0.4 M ammonium acetate. SDS was added to a final concentration of 1%, followed by heating at 65 °C for 10 min. Samples were cooled on ice and 1 ml of immunoprecipitation buffer was added to dilute the SDS. HA antibody was added to the mixture and incubated overnight, and material was captured using protein G-Sepharose. Following washes with IP buffer, proteins were released from the beads via the addition of 1× sample buffer with or without 50 mM dithiothreitol.

GFP Studies—GFP microscopy was performed as described (36). FBPase-GFP or Sec28p-GFP were transformed into cells using the PCR-based integration methods described by Longtine *et al.* (45). The PCR was performed using the primers listed in Table 2. Cells were grown under YPKG conditions to induce FBPase. In most studies, cells were shifted to glucose in the presence of the FM 4-64 dye for various periods of time. In some experiments, cells were preincubated with FM 4-64 for 1 h and chased in YPKG without the dye overnight. These cells were then shifted to glucose for various periods of time. Cells were examined using a Zeiss Axiovert s100 (Carl Zeiss Inc., Thornwood, NY) fluorescence microscope and images were taken with a digital camera (Hamamatsu Inc., Japan).

Immunofluorescence Microscopy— Δ *vam3* cells expressing Vid24p-HA were grown in YPKG to induce FBPase. Cells were then shifted to glucose for 30 min and spheroplasted with zymolase. Cells were incubated with anti-HA antibodies at 1:10 dilution or anti-Sec28p antibodies at 1:10 dilution followed by Texas Red-conjugated goat anti-mouse secondary antibodies or fluorescein isothiocyanate-conjugated goat anti-rabbit antibodies at 1:50 dilution. Cells were washed and visualized using fluorescence microscope equipped with a digital camera.

RESULTS

SEC28 Is Required for the Vacuolar Pathway of FBPase Degradation—In an attempt to identify molecules that are involved in FBPase degradation and Vid vesicle function, two different approaches were used. The first one utilized genome-wide screening of a deletion library where individual open reading frames were disrupted. Strains that failed to degrade FBPase following a shift to glucose were identified using a colony blot procedure (30). One strain that showed a severe FBPase degradation defect was the Δ *sec28* mutant. *SEC28* encodes the ϵ -COP component of the COPI coatomer, a complex that has a known role in vesicular transport from the Golgi to the ER, as well as endocytic trafficking (3–5, 7, 16–21). In a second approach, Vid vesicles were purified using established protocols (36) and proteins from the Vid vesicle fractions were subjected to MALDI analysis. A number of proteins were identified using this approach. These included Sec28p, as well as other subunits of the COPI coatomer complex such as Sec21p and Ret1p.

We have shown that FBPase is degraded in the proteasome when glucose is added to cells that are starved for 1 day. In

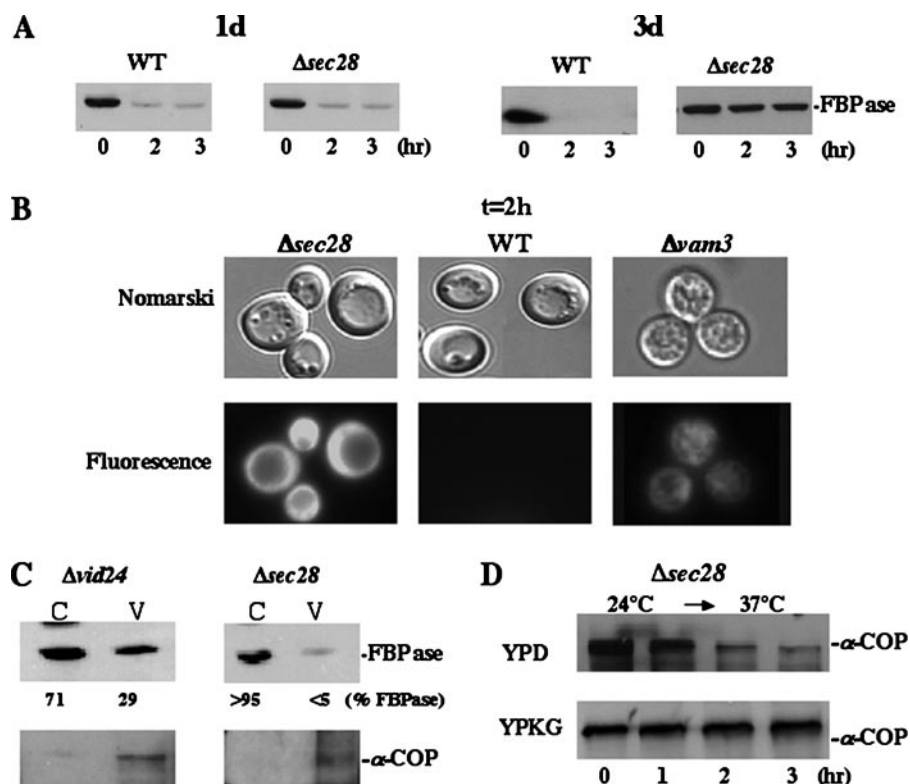


FIGURE 1. SEC28 is required for the vacuole-dependent FBPAse degradation pathway. *A*, wild type and $\Delta sec28$ strains were grown in YPKG media for 1 or 3 days to induce FBPAse. FBPAse degradation was examined after cells were shifted to glucose for 0, 2, and 3 h. *B*, wild type, $\Delta sec28$, and $\Delta vam3$ strains expressing FBPAse-GFP were grown in YPKG media for 3 days and then shifted to fresh glucose media for 2 h. Fluorescence microscopy was used to determine the localization of FBPAse-GFP. *C*, $\Delta vid24$ and $\Delta sec28$ strains were glucose starved and then shifted to high glucose media for 30 min. Cells were homogenized and subjected to differential centrifugation as described previously (37). The resultant cytosol (C) and vesicles (V) were examined for the distribution of FBPAse and α -COP. *D*, $\Delta sec28$ cells were grown in YPD or YPKG at 24 °C and shifted to glucose at 37 °C for 0–3 h. The levels of α -COP were examined.

contrast, when 3-day starved cells are shifted to glucose, FBPAse is degraded in the vacuole (36). Therefore, to test whether SEC28 functions in the vacuolar pathway or proteasome pathway, the $\Delta sec28$ strain was starved of glucose for either 1 or 3 days. Cells were then shifted to fresh glucose and examined for FBPAse degradation. For 1-day starved $\Delta sec28$ cells, FBPAse was degraded at a rate similar to that seen in wild type cells (Fig. 1A). By contrast, when 3-day starved $\Delta sec28$ cells were shifted to glucose, FBPAse degradation was blocked (Fig. 1A). Therefore, SEC28 is not involved in the proteasome-dependent pathway, but is needed for the vacuolar dependent pathway.

SEC28 Plays a Role in the Import of FBPAse into Vid Vesicles—For the vacuolar-dependent degradation pathway, FBPAse is imported into intermediate carriers known as Vid vesicles (36). If SEC28 is involved in either FBPAse import into Vid vesicles or in the formation of Vid vesicles, FBPAse should accumulate in the cytosol in the $\Delta sec28$ mutant. In contrast, if SEC28 plays a role downstream of FBPAse import, a portion of FBPAse should accumulate in Vid vesicles. FBPAse-GFP was expressed in wild type and $\Delta sec28$ cells and these strains were shifted to glucose for 2 h (Fig. 1B). Following a 2-h shift to glucose, most of the FBPAse-GFP was in the cytosol in $\Delta sec28$ cells. By contrast, wild type cells degraded FBPAse after a glucose shift for 2 h. Therefore, in the $\Delta sec28$ mutant, the trafficking of FBPAse appears to be blocked prior to import of this protein into Vid vesicles. This

was not the case, however, for the $\Delta vam3$ mutant. This mutant also blocks FBPAse degradation, but the block occurs after FBPAse is imported into Vid vesicles. Accordingly, when this strain was examined following a shift to glucose for 2 h, a portion of FBPAse was seen in punctuate structures. Note, however, that the $\Delta vam3$ mutant also contained high levels of FBPAse in the cytosol. This distribution was as expected, and it is consistent with fractionation data for this same mutant (see Fig. 3B).

To further confirm the site of the degradation defect in $\Delta sec28$ cells, differential centrifugation was performed. The $\Delta vid24$ strain was used for comparative purposes in these experiments, because this strain accumulates FBPAse in the Vid vesicle fraction. The $\Delta vid24$ and $\Delta sec28$ cells were glucose starved and shifted to glucose for 30 min. In $\Delta vid24$ cells, FBPAse was detected in the cytosol (200,000 \times g supernatant) as well as the vesicle (200,000 \times g pellet) fractions (Fig. 1C). However, in the $\Delta sec28$ mutant, the vast majority of FBPAse was in the cytosolic fraction. Thus, our results suggest that SEC28 is

required for FBPAse association with Vid vesicles. As an experimental control, we examined the distribution of α -COP under the same condition. The majority of this protein was detected in the Vid vesicle fractions. Interestingly, the stability of α -COP was not affected in cells lacking the SEC28 gene under our YPKG conditions (Fig. 1D). In contrast, α -COP was unstable when the $\Delta sec28$ mutant was grown under the YPD-rich medium (Fig. 1D and Ref. 42). Thus, the stability of α -COP appears to vary depending on growth conditions.

Sec28p Is a Component of Vid Vesicles—As mentioned above, Sec28p was identified as a component of Vid vesicles based on our MALDI analysis. To verify that Sec28p is indeed a component of Vid vesicles, we performed co-localization experiments using subcellular fractionation as well as indirect immunofluorescence. For fractionation experiments, $\Delta vam3$ cells were used, because these mutants accumulate Vid vesicles to a higher level than wild type strains (41). Cell lysates were subjected to differential centrifugation followed by sucrose density gradient separation procedures. Sec28p was distributed in both light density (fractions 2–4) and heavy density fractions (fractions 6–8 and 9–12) (Fig. 2A). We have shown that fractions 2–4 are heterogeneous and contained multiple organelle markers, whereas fractions 9–12 contained Vid vesicles (36). Fractions 6–8 have not been characterized previously and they may represent

The Vid Degradation Pathway Merges with the Endocytic Pathway

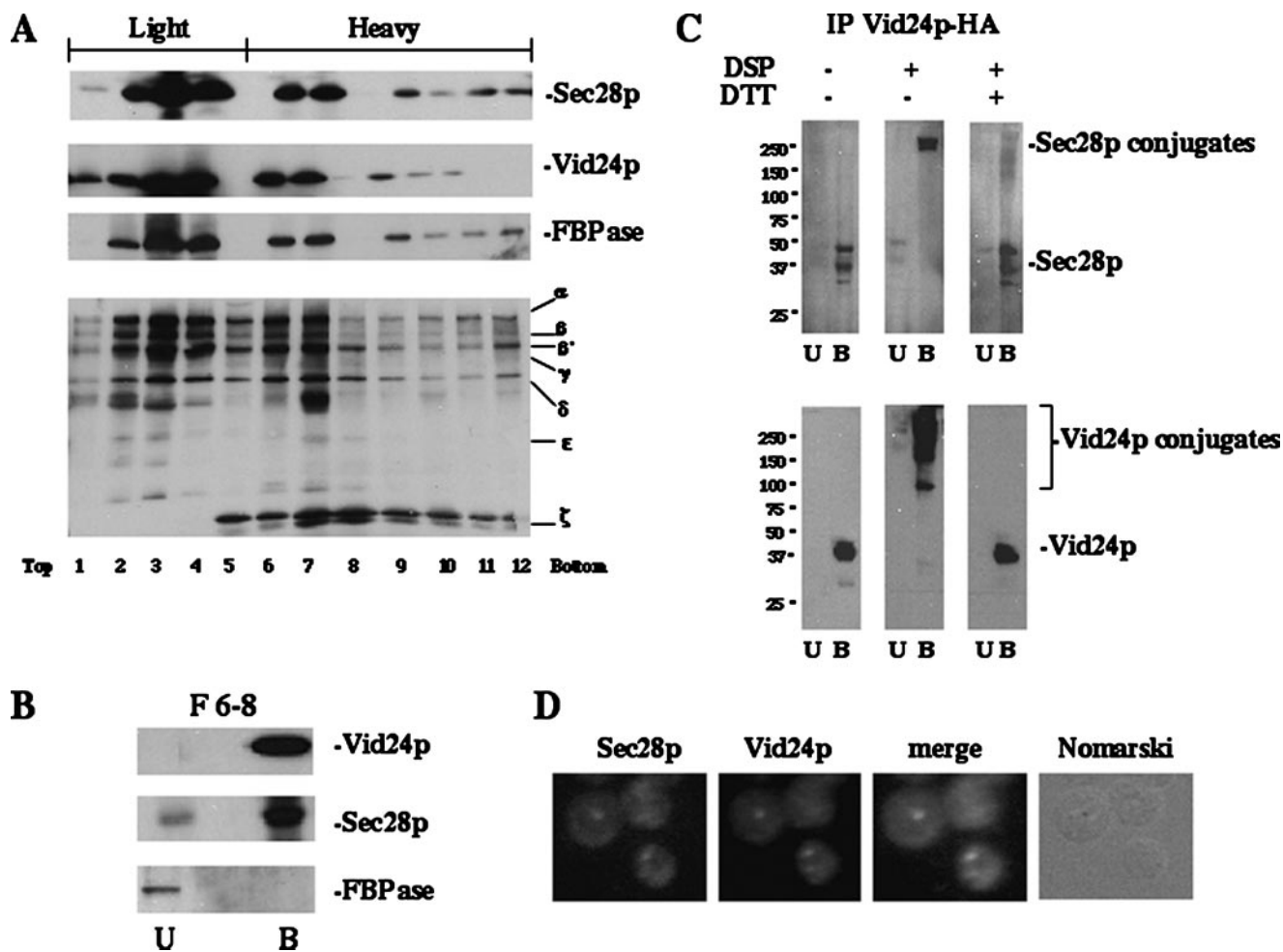


FIGURE 2. Sec28p co-localizes with Vid24p. *A*, the $\Delta vam3$ strain expressing Vid24p-HA was shifted to glucose for 30 min and harvested. Cell lysates were subjected to differential centrifugation followed by sucrose density gradient analysis. Fractions were collected from the top and concentrated by trichloroacetic acid precipitation. Samples were then immunoblotted with antibodies directed against Sec28p, Vid24p-HA, FBPase, and coatomer proteins. *B*, fractions 6–8 were pooled and solubilized with Triton X-100. Vid24p was precipitated with anti-HA antibodies. The resultant unbound and bound fractions were immunoblotted with HA, Sec28p, and FBPase antibodies. *U*, Unbound fractions; *B*, bound fractions. *C*, wild type cells were shifted to glucose for 30 min. Lysates were subjected to differential centrifugation followed by sucrose density gradient. The Vid vesicle-enriched fractions were treated with or without DSP. Samples were immunoprecipitated with HA antibodies under denaturing conditions followed by capture with protein G beads. Samples were treated with or without dithiothreitol (DTT). The bound and unbound fractions were blotted with anti-Sec28p and anti-HA antibodies. *D*, the $\Delta vam3$ mutant expressing Vid24p-HA was glucose shifted for 30 min and immunofluorescence was performed. Vid24p-HA was detected using monoclonal anti-HA antibodies and rhodamine-conjugated goat anti-mouse secondary antibodies. Sec28p was detected using purified rabbit anti-Sec28p antibodies and fluorescein isothiocyanate-conjugated goat anti-rabbit antibodies.

Vid vesicles with different densities. They may also contain Vid vesicle precursor membranes or compartments derived from Vid vesicles, because both Vid24p and FBPase were found in these fractions. On the sucrose density gradient, FBPase and Vid24p showed the same distribution profile as Sec28p, offering further evidence that Sec28p associates with multiple organelles including Vid vesicles.

Because Sec28p and Vid24p are distributed in similar fractions, we examined whether there was an interaction between these proteins. $\Delta vam3$ mutant cells expressing Vid24p-HA were starved for 3 days and then shifted to glucose for 30 min. Sucrose gradients were performed and fractions 6–8 were pooled, detergent solubilized, and immunoprecipitated with anti-HA antibodies. The precipitated material was then immunoblotted with Sec28p antibodies. As shown in Fig. 2*B*, Sec28p was in the bound fraction that was precipitated with Vid24p, suggesting that there was an interaction between Sec28p with

Vid24p. Interactions were also observed using samples from fractions 2–4 or 9–12 (not shown).

Interaction of Sec28p with Vid24p was also detected in wild type cells, when these proteins were cross-linked with the cross-linking agent DSP. (Fig. 2*C*). Vid vesicles were isolated using differential centrifugation followed by sucrose gradients. Samples were treated with DSP and immunoprecipitated with HA antibodies under denaturing conditions followed by capture with protein G beads. Proteins were separated into unbound and bound fractions and treated with or without the reducing agent dithiothreitol. In the absence of DSP, most of the Sec28p and Vid24p were detected in the bound fraction. Upon DSP treatment, however, both proteins were detected on the top of the SDS gel in the bound fraction, indicating that they form a large complex. When dithiothreitol was added to the DSP-treated sample, Vid24p and Sec28p were reduced and they migrated at their corresponding positions on the SDS gel.

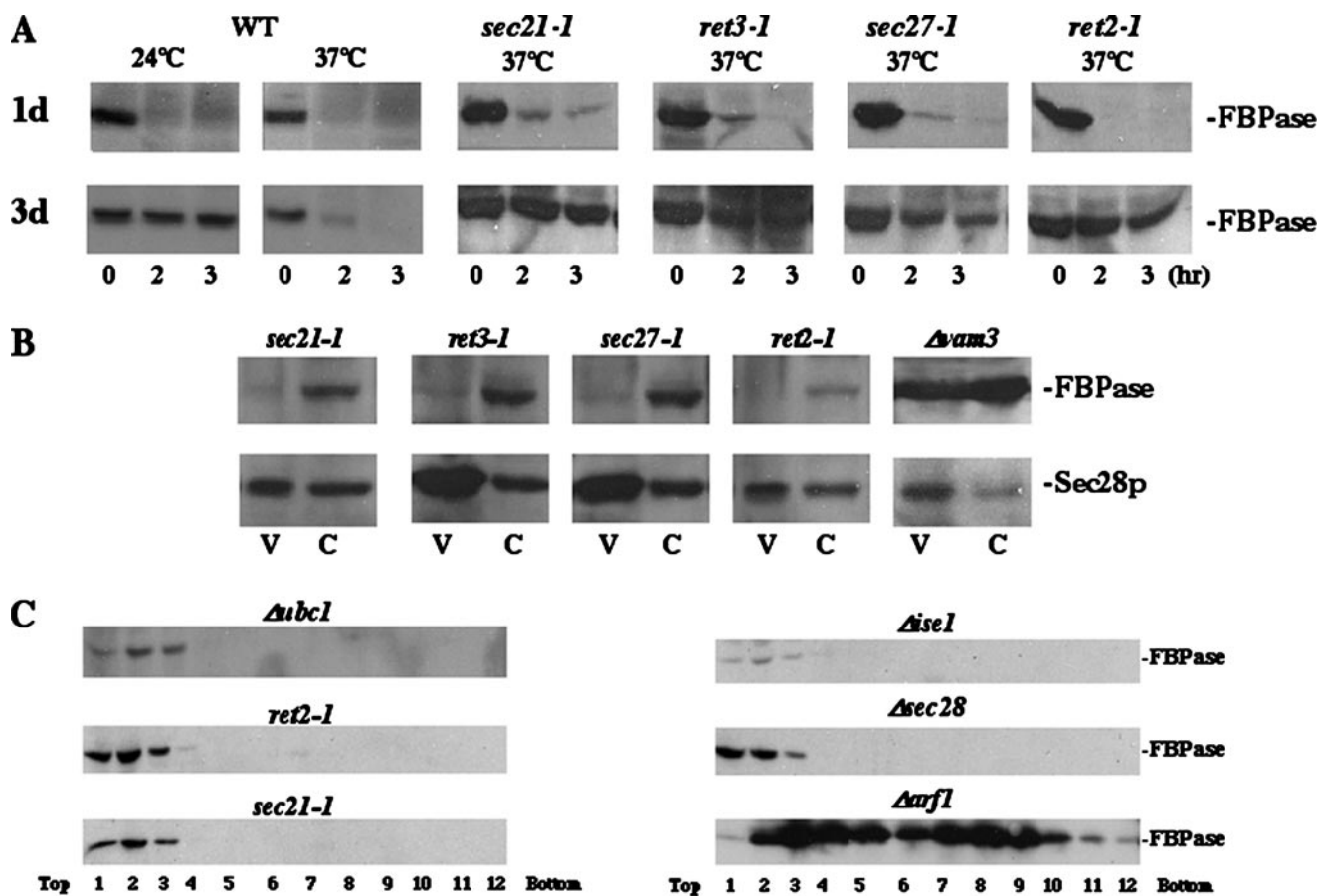


FIGURE 3. **FBPase degradation is defective in coatomer mutants.** *A*, wild type and coatomer mutants (*sec21-1*, *ret3-1*, *sec27-1*, and *ret2-1*) were starved in YPKG media for either 1 or 3 days at 24 °C to induce FBPase. Wild type cells were shifted to glucose at either 24 or 37 °C, whereas coatomer mutants were shifted to glucose at 37 °C for 0–3 h. Cells were harvested and FBPase degradation was examined. *B*, coatomer mutants and $\Delta vam3$ cells were shifted to glucose at 37 °C and then fractionated. The distribution of FBPase and Sec28p was examined in Vid vesicle and cytosolic fractions. *C*, mutant strains ($\Delta ubc1$, *ret2-1*, *sec21-1*, $\Delta ise1$, $\Delta sec28$, and $\Delta arf1$) were shifted to glucose for 30 min and lysates were subjected to differential centrifugation followed by sucrose density gradient analysis. FBPase distribution was examined by immunoblotting.

Vid24p may also interact with other proteins, because this protein appeared as a smear on the top of the gel upon DSP treatment. In addition, a significant fraction of Vid24p failed to enter the gel.

Finally, we characterized Sec28p-Vid24p localization using microscopic studies. Initially, we attempted to produce Vid24p-RFP and co-express it with cells containing Sec28p-GFP. However, the Vid24p-RFP signal was below detection. Therefore, as an alternative approach, we performed indirect immunofluorescence using $\Delta vam3$ cells expressing Vid24p-HA. A portion of Sec28p was observed in structures that were likewise stained with the Vid vesicle marker protein Vid24p (Fig. 2D). Thus, taken together, the immunofluorescence and density gradient experiments further strengthened our conclusion that Sec28p is a component of Vid vesicles.

FBPase Degradation Is Defective in Coatomer Mutants—Sec28p is a subunit of the coatomer protein complex found on COPI vesicles. Therefore, it is possible that other coatomer components play a role in FBPase degradation. Coatomer proteins in yeast include α , β , β' , γ , δ , ϵ , and ζ subunits, and these proteins are encoded by the *RET1*, *SEC26*, *SEC27*, *SEC21*, *RET2*, *SEC28*, and *RET3* genes, respectively (13, 21, 42, 43). Because each of these genes is essential, except *SEC28*, we examined their roles in FBPase degradation using temperature-

sensitive mutants. Note that the *ret1* strains grew poorly under prolonged starvation conditions and they were not used for these studies. When coatomer mutants were starved for 1 day and shifted to glucose at 37 °C, FBPase was degraded normally (Fig. 3A), suggesting that coatomers are not involved in FBPase degradation in the proteasome pathway. By contrast, when these mutants were starved for 3–4 days and then shifted to glucose at 37 °C, FBPase degradation was defective, although the degree of defects varied from strain to strain (Fig. 3A). Thus, most coatomer proteins appear to be required for FBPase degradation in the vacuole. It should be noted that FBPase degradation is sensitive to temperature for 3-day starved cells. Wild type cells that were starved for 3 days showed retarded degradation at 24 °C. Therefore, 3-day starved coatomer mutants and wild type cells were shifted to glucose at 37 °C for subsequent experiments.

To determine whether coatomer genes played a similar role as *SEC28*, we examined FBPase distribution in these mutants. The majority of this protein was in cytosolic fractions (Fig. 3B), suggesting that mutations of these genes blocked the same step of the FBPase degradation pathway as $\Delta sec28$. As a loading control, we also examined the distribution of Sec28p. As expected, a high percentage of this protein was detected in the Vid vesicle-enriched fractions in these strains.

The Vid Degradation Pathway Merges with the Endocytic Pathway

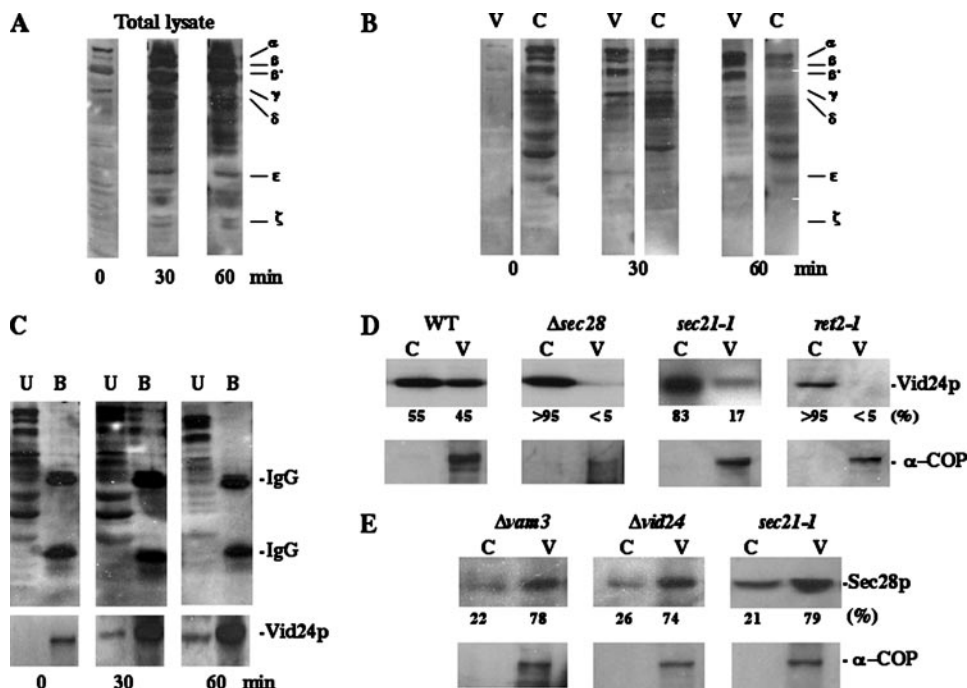


FIGURE 4. Vid24p interacts with coatomer. *A*, wild type cells expressing Vid24p-HA were glucose starved and then shifted to glucose for 0, 30, and 60 min. Levels of coatomer proteins in total lysates were determined by immunoblotting. *B*, lysates were further separated into vesicle (V) and cytosol (C) fractions. The amounts of coatomer proteins in each fraction were determined by Western blotting. *C*, Vid vesicle fractions were solubilized with Triton X-100 and immunoprecipitated with HA antibodies. The unbound and bound fractions were immunoblotted with anti-HA and anti-coatomer antibodies. *D*, wild type, $\Delta sec28$, $sec21-1$, and $ret2-1$ strains were grown in YPKG at 24 °C and cells were shifted to glucose at 37 °C for 30 min. The distributions of Vid24p and α -COP in the cytosol and Vid vesicle-enriched fractions were examined in these mutants. *E*, Sec28p and α -COP distributions in the cytosol and Vid vesicle-enriched fractions of $\Delta vam3$, $\Delta vid24$, and $sec21-1$ cells were determined.

To confirm the above results, we studied the FBPase distribution profile in coatomer mutants using sucrose density gradients. FBPase was distributed primarily in the light fractions in these mutants, whereas levels were significantly decreased in heavy fractions (Fig. 3C) as compared with $\Delta vam3$ cells (see Fig. 2A). Note that FBPase distribution in coatomer mutants was similar to cells lacking *UBC1* (ubiquitin-conjugating enzyme) and in cells lacking *ISE1* (also called *ERG6*, a gene encoding the Δ sterol C-methyltransferase involved in the ergosterol biosynthetic pathway). Because these strains are defective in the formation of Vid vesicles (34), this suggests that coatomer genes play a role in Vid vesicle biogenesis. Interestingly, a different pattern was observed for the $\Delta arf1$ mutant. Although the *ARF1* (ADP-ribosylation factor) gene plays a major role in regulating the formation of COPI vesicles (46, 47), FBPase was degraded normally in the $\Delta arf1$ mutant (not shown). Furthermore, following sucrose density gradient fractionation, FBPase distribution was extended into heavy fractions, suggesting that *ARF1* does not play a major role in FBPase degradation or Vid vesicle formation.

Vid24p Interacts with Coatomer Proteins—Because Sec28p resides on Vid vesicles, other coatomer proteins may also exhibit similar localization. Indeed, coatomer proteins showed an identical sucrose gradient distribution pattern as Sec28p, Vid24p, and FBPase (see Fig. 2A). In wild type cells, coatomer proteins were present at low levels in lysates isolated prior to a glucose shift ($t = 0$ min), but these levels increased significantly

following a shift to glucose for 30 or 60 min (Fig. 4A). When total lysates were further fractionated into cytosol-enriched and Vid vesicle-enriched fractions, the levels of coatomer proteins in Vid vesicle fractions increased following a glucose shift (Fig. 4B).

As shown above (Fig. 2), Sec28p interacts with Vid24p. Therefore, we next tested whether coatomer proteins form a similar complex with Vid24p. Wild type expressing Vid24p-HA were starved for 3 days and then shifted to glucose for 0, 30, and 60 min. The Vid vesicle-enriched fractions were isolated, detergent solubilized, and immunoprecipitated with anti-HA antibodies. The bound and unbound materials were then immunoblotted with antibodies produced against coatomers. As shown in Fig. 4C, little interaction was observed at $t = 0$. However, at $t = 30$ min, a fraction of coatomer proteins were precipitated with Vid24p in the bound fraction, indicating that coatomer proteins and Vid24p interact. Interestingly, the interaction between coatomer and Vid24p was reduced

at $t = 60$ min. Because a portion of Vid vesicles may have already fused with downstream compartments at this time point, less interaction may be due to lower levels of Vid24p and/or a lower number of Vid vesicles present at this time.

Our interaction and fractionation data suggest that Vid24p, Sec28p, and coatomer proteins are part of a large protein complex on Vid vesicles. As such, the absence of one of these proteins may affect the ability of the other proteins to localize to Vid vesicles. Along these lines, the $\Delta sec28$ strain had reduced levels of Vid24p in the Vid vesicle fraction as compared with the wild type strain (Fig. 4D). The $sec21-1$ and $ret2-1$ mutants also showed decreased amounts of Vid24p in the Vid vesicle fraction. These results suggest that coatomer proteins play a role in Vid24p association with Vid vesicles. By contrast, Vid24p does not appear to be required for coatomer association with Vid vesicles. Sec28p levels remained high in Vid vesicle fractions, isolated from cells lacking Vid24p and Vam3p as well as in the $sec21-1$ cells (Fig. 4E). Under the same conditions, most of the α -COP was also found in the Vid vesicle fractions (Fig. 4, D and E).

Sec28p Traffics to Endocytic Compartments in Wild Type Cells—Although FBPase degradation utilizes a highly selective pathway, we have data suggesting that the endocytosis pathway is also involved in this process. For example, several endocytosis mutants are defective in FBPase degradation. Furthermore, a role for Sec28p and coatomer proteins in endocytosis in mammalian cells has been demonstrated (16–20). In yeast, a sub-

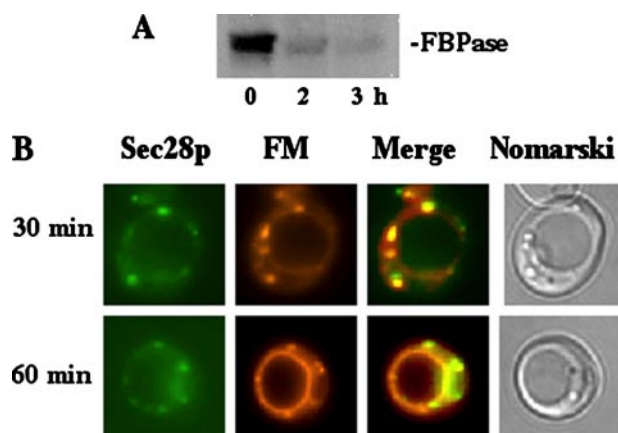


FIGURE 5. **Sec28p merges with the endocytic pathway.** *A*, wild type cells expressing Sec28p-GFP were glucose starved and then shifted to glucose for 0, 2, and 3 h. FBPase degradation was examined. *B*, wild type cells expressing Sec28p-GFP were shifted to glucose in the presence of FM 4-64. At the indicated time points, cells were harvested and Sec28p and FM staining was visualized by fluorescence microscopy. Cells were visualized using Nomarski optics.

complex of coatomer proteins, including Sec28p, was recently shown to be involved in protein sorting in the multivesicular body (21).

To clarify the role that endocytosis may play in our degradation pathway, we performed experiments following the kinetics of uptake of the lipophilic dye FM 4-64 (48). FM 4-64 is internalized, moving from the plasma membrane to endosomes, before finally reaching the vacuole. To track the Vid vesicle trafficking pathway, we also followed the distribution of Sec28p in various mutant strains. Note that other coatomer proteins are likely to exhibit the same distribution as Sec28p, because they form a protein complex with Sec28p, and they were all detected in the Vid vesicle fractions. Sec28p-GFP was integrated into the *SEC28* locus by homologous recombination. This integration did not interfere with Sec28p function, because FBPase was degraded normally in wild type cells expressing Sec28p-GFP (Fig. 5*A*). We observed that a significant fraction of Sec28p localized with FM at early time points in wild type cells (Fig. 5*B*), suggesting that Sec28p traffics to FM containing endosomes.

Because FM uptake has not been examined under our experimental conditions, we determined FM uptake kinetics in wild type cells, as well as in various mutants that block the FBPase degradation pathway (Fig. 6). In wild type cells, FM was observed in dots representing endosomes at early time points following a glucose shift, and then in large circles representing vacuoles at 1–2 h. During the first 60 min, we frequently observed 1–3 large circles in wild type cells (Fig. 6*A*). In contrast, we found two different phenotypes of FM uptake in mutants that affect the FBPase degradation pathway (Fig. 6*B*). Cells lacking Ypt7p (a small GTPase) or Vam3p (vacuole t-SNARE) displayed numerous smaller FM containing circles/dots. Other mutants, such as cells lacking Sec28p, Vid24p, Ubc1p, or Vph1p (100 kDa subunit of vacuolar ATPase), displayed multiple large circles. The small circles/dots resembled vacuoles that accumulate in class C *vps* mutants, whereas large circles resembled vacuoles that accumulate in class B *vps* mutants (49, 50). Based on these results, mutants from each of

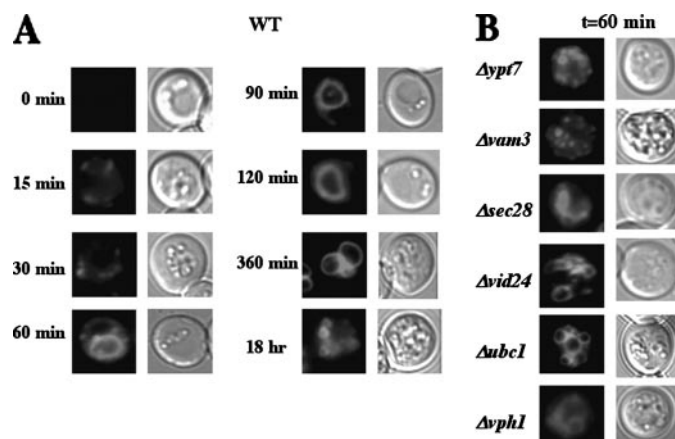


FIGURE 6. **Distribution of FM 4-64 in wild type and mutant strains grown under glucose starvation conditions.** *A*, wild type cells were shifted to glucose media containing FM 4-64 for the indicated periods of time. *B*, various mutants were shifted to glucose media plus FM 4-64 for 1 h. Localization of FM was observed using fluorescence microscopy.

these groups were transformed to express Sec28p-GFP and utilized for further studies. Note that during prolonged glucose starvation, the vacuole occupies ~90% of cell volume. Hence, results obtained from prolonged starved cells were difficult to interpret. To overcome this problem, cells with smaller vacuoles or with vacuoles on one side of the cell were chosen for analysis.

Sec28p Does Not Converge with the Endocytic Pathway in Cells Lacking the VAM3 Gene—In the wild type cell, a portion of Sec28p co-localizes with FM containing endosomes after a glucose shift (see Fig. 5*B*), suggesting that Sec28p traffics to the endocytic compartments. To identify the gene(s) that control the trafficking of Sec28p to the endocytic pathway, we screened FBPase degradation deficient mutants and examined the distribution of Sec28p and FM in these strains. As mentioned above, the absence of the *VAM3* gene results in the accumulation of numerous small FM containing circles (Fig. 6*B*). When we examined Sec28p distribution in $\Delta vam3$ (Fig. 7*A*), we did not observe obvious co-localization of Sec28p with the FM dye, suggesting that the movement of Sec28p to endocytic compartments is blocked in this strain. This raises an interesting possibility. Namely, convergence of the Vid and endocytic pathways may be controlled by the *VAM3* gene.

Sec28p Is on the Vacuole Membrane in Cells Lacking the UBC1 Gene—The *UBC1* gene plays an important role in Vid vesicle formation (34). As such, in the absence of *UBC1*, FBPase remains in the cytosol, and the levels of Vid vesicles are reduced (34). Given that coatomer proteins are involved in the budding of COPI vesicles, they may play a similar role in the formation of Vid vesicles. If this is the case, Sec28p may selectively localize to one of the Vid vesicle precursor membrane(s) in the absence of *UBC1*. At early times following glucose shift, Sec28p was seen in dots that co-localized with the FM dye in cells lacking this gene (Fig. 7*B*). At later time points, however, this protein was found primarily on vacuole membranes that also labeled with FM dye. These results suggest that Sec28p anterograde transport to the vacuole is not affected in the absence of *UBC1*. However, Sec28p remained on the vacuole membrane for a pro-

The Vid Degradation Pathway Merges with the Endocytic Pathway

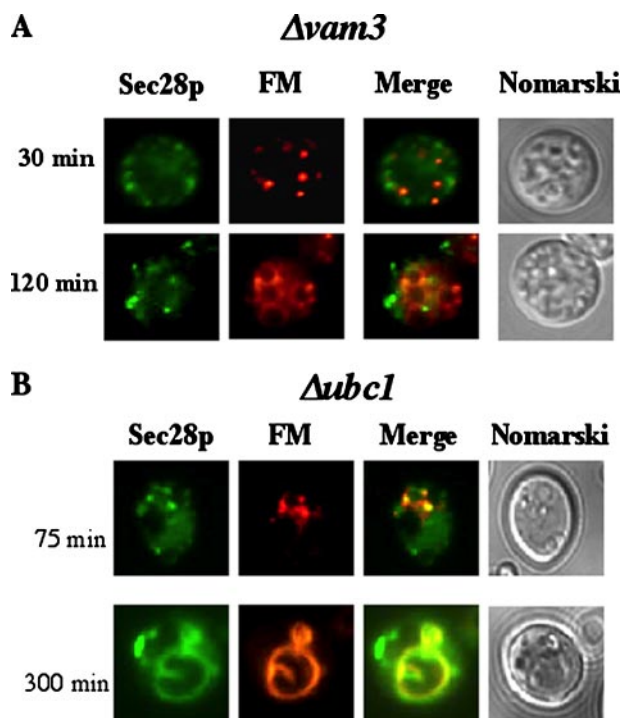


FIGURE 7. Sec28p does not co-localize with FM in $\Delta vam3$ cells, but it localizes to the vacuolar membrane in $\Delta ubc1$ cells. *A*, $\Delta vam3$ mutants expressing Sec28p-GFP were glucose starved and then shifted to glucose media with FM for the indicated times. Sec28p, FM, and cells were examined. *B*, Sec28p and FM distributions were examined in $\Delta ubc1$ cells that were shifted to glucose for the indicated times.

longed period of time following the arrival of Sec28p on the vacuole membrane.

Sec28p and Vacuole Membrane Dynamics—Because Sec28p is part of the coatamer protein complex, mutations of other coatamer genes may affect the distribution of Sec28p, perhaps resulting in its retention at the site of vesicle budding in one of the precursor membrane(s). In the *ret2-1* mutant, Sec28p co-localized with FM at earlier time points (not shown). However, at $t = 180$ min, FM dye was on the vacuolar membrane, whereas Sec28p was in dots adjacent to or on the vacuole membrane (Fig. 8A). The localization of Sec28p and FM in dots near or on the vacuole membrane could represent vesicles that are in the process of fusing with the vacuolar membrane. Alternatively, they may be vesicles that are budding from the vacuolar membrane. To address this, we pre-labeled the vacuolar membrane with FM dye. The FM was removed, and cells were then chased in the absence of FM for 18 h. Cells were then shifted to glucose containing media for the indicated periods of time. Co-localization of Sec28p in dots on the vacuole membrane was observed after 60–120 min of glucose shift (Fig. 8B). Thus, these data suggest that Sec28p containing vesicles can form from the vacuolar membrane.

FBPase and the Endocytic Pathway—The above data indicate that the Vid and endocytic pathways overlap. In particular, Sec28p was associated with endocytic structures in wild type and $\Delta ubc1$ mutants following glucose shift. However, Sec28p does not associate with FM 4-64-labeled structures in $\Delta vam3$ cells. Based on these data, we suggest that the *VAM3* gene controls the merger of the Vid pathway with the endocytic path-

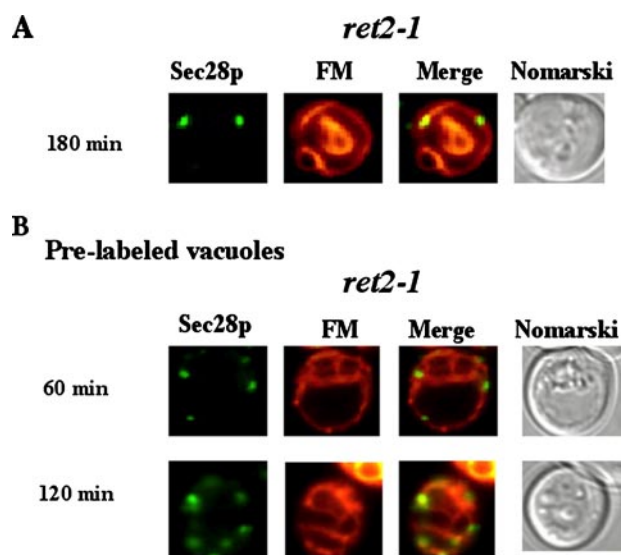


FIGURE 8. Sec28p localizes to vesicles on the vacuolar membrane in the *ret2-1* mutant. *A*, *ret2-1* cells were shifted to glucose media containing FM for 180 min and examined for Sec28p and FM distributions. *B*, vacuoles were pre-labeled with FM in *ret2-1* cells. Glucose was then added for the indicated times, after which Sec28p and FM distributions were examined.

way. If this is true, FBPase should remain in Vid vesicles in cells lacking this gene. To test this idea, we followed FBPase distribution in the $\Delta vam3$ mutant. We found that the majority of FBPase was in punctate structures that did not show obvious co-localization with FM (Fig. 9A). This further supports our conclusion that the *VAM3* gene controls the convergence of the Vid pathway with the endocytic pathway.

If our model is correct, whereby Vid vesicle trafficking merges with the endocytic system, then we would expect to see some co-localization or co-fractionation of the FBPase cargo with endocytic compartments. To further investigate this connection, we used the $\Delta vph1$ strain, because this strain displays small FM dots at earlier time points and accumulates large FM-labeled circles at later time points (Fig. 9B, *FM images*). In this strain, FBPase-GFP was diffuse in the cytoplasm prior to glucose shift. At $t = 25$ min, however, a fraction of FBPase was observed in punctate structures that were stained with the FM dye. Localization of FBPase in FM containing structures was observed following a shift to glucose for a longer period of time (Fig. 9B).

To support the idea that the FBPase pathway is linked to the endocytic pathway, we used a $\Delta pep4$ strain that is deficient in vacuole proteolysis. Cells were shifted to glucose for 30 min and cell lysates were subjected to differential centrifugation. High-speed pellets were then fractionated on an S-1000 size column. These fractions were then blotted with FBPase antibodies (Fig. 9C). Multiple FBPase containing peaks were found; peak A (fractions 11–14), peak B (15–18), peak C (19–22), and peak D (23–30). Peak D had the highest amounts of FBPase and these fractions were previously characterized as containing Vid vesicles (36). Although the amounts of FBPase in peaks B and C were lower than the other peaks, these fractions also contained the late endosome marker Pep12p, suggesting that at least a portion of FBPase co-localizes with endocytic compartments. Note that Pep12p was below the level of detection in the Vid

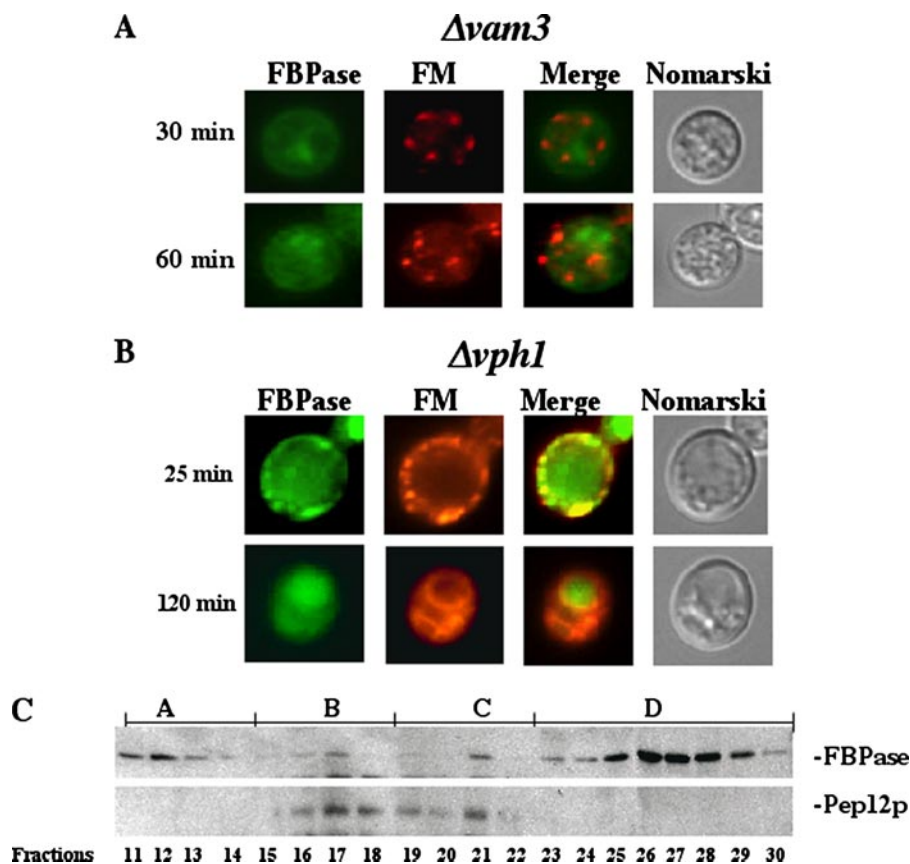


FIGURE 9. FBPase does not co-localize with FM in the $\Delta vam3$ mutants, but it co-localizes with endocytic compartments in $\Delta vph1$ cells. *A*, $\Delta vam3$ mutants expressing FBPase-GFP were shifted to glucose in the presence of FM for the indicated times. The distribution of FBPase, and FM were visualized and merged. *B*, $\Delta vph1$ cells expressing FBPase-GFP were shifted to glucose in the presence of FM for the indicated times. The distribution of FBPase and FM was examined and merged. *C*, $\Delta pep4$ cells were shifted to glucose for 30 min and lysates were subjected to differentiation centrifugation. High-speed pellets were fractionated on an S-1000 column. Fractions were precipitated with trichloroacetic acid and proteins were resolved using SDS-PAGE. The distribution of FBPase and Pep12p was examined via Western blotting.

vesicle containing fractions in peak D. Taken together, these results offer further support that FBPase utilizes the endocytic pathway for its delivery to the vacuole.

DISCUSSION

In our study, we showed that *SEC28* and COPI coatomer genes play an important role in the FBPase degradation pathway. Initially, the *SEC28* gene was identified in our genetic screen for mutants defective in the degradation of FBPase. In conjunction with these studies, various coatomer proteins, including Sec28p, were identified from purified Vid vesicles following MALDI analysis of proteins. Each of the coatomer genes was necessary for the association of FBPase with the Vid vesicle fraction. In addition, coatomer proteins are components of Vid vesicles and they form a protein complex with Vid24p. When coatomer genes were mutated, Vid24p association with Vid vesicles was reduced, suggesting that coatomer proteins play a role in recruiting Vid24p to Vid vesicles.

Previously, Sec28p was shown to localize to endocytic compartments in both mammalian cells and yeast (16–21). Our studies extended these earlier reports, showing that Sec28p localizes to multiple locations along the endocytic pathway. Sec28p co-localized with the FM dye in small circles/dots in

wild type and $\Delta ubc1$ cells at earlier time points. These small circles/dots may represent endosomes because they were observed at earlier time points. At later time points, Sec28p was seen on the vacuole membrane in the $\Delta ubc1$ mutant. This protein was also detected in multiple discrete foci on the vacuole membrane in the *ret2-1* mutant. Taken together, these data offer strong evidence suggesting that the Sec28p traffics to the endocytic pathway.

Although the Vid vesicle pathway appears to merge with the endocytic pathway, our data indicate that this merger may be controlled by the *VAM3* gene. In the $\Delta vam3$ mutant, there was no clear co-localization of Sec28p with FM, suggesting that Sec28p does not enter the endocytic pathway in the absence of this gene. The vesicle-like structures seen in the $\Delta vam3$ mutants are unlikely to be individual Vid vesicles, because these vesicles are too small to be seen using fluorescence microscopy. However, Vid vesicles can cluster and form larger structures that can be easily identified with this technique. Whether these clusters are Vid vesicles that adhere to each other loosely or whether they are surrounded by membrane(s) is currently unknown.

Based on our studies, we propose the following model for the Sec28p trafficking pathway (Fig. 10). For anterograde trafficking, Sec28p resides on Vid vesicles, and these vesicles ultimately converge with the endocytic pathway. The *VAM3* gene regulates this convergence, and in its absence, Sec28p remains associated with Vid vesicles. Following the fusion of endosomes with the vacuole, Sec28p is distributed on the vacuolar membrane. Finally, Sec28p concentrates in buds that pinch off from the vacuole membrane. The *UBC1* gene likely controls the formation of Sec28p vesicles on the vacuole membrane. As such, in the absence of this gene, Sec28p is distributed evenly on the vacuolar membrane. The *RET2* gene most likely is involved in the pinching off of vesicles. For example, Sec28p was observed in vesicles that appeared to be associated with the vacuole membrane in the *ret2-1* mutant when the vacuole was pre-labeled in this strain. These Sec28p containing retrograde vesicles may become Vid vesicles later, or alternatively, they may travel to the plasma membrane and become Vid vesicles following internalization of the plasma membrane.

Finally, our data are consistent with a model in which FBPase is transported to the vacuole via the endocytic pathway. In the $\Delta vph1$ mutant, FBPase was initially in the cytosol and appeared in

The Vid Degradation Pathway Merges with the Endocytic Pathway

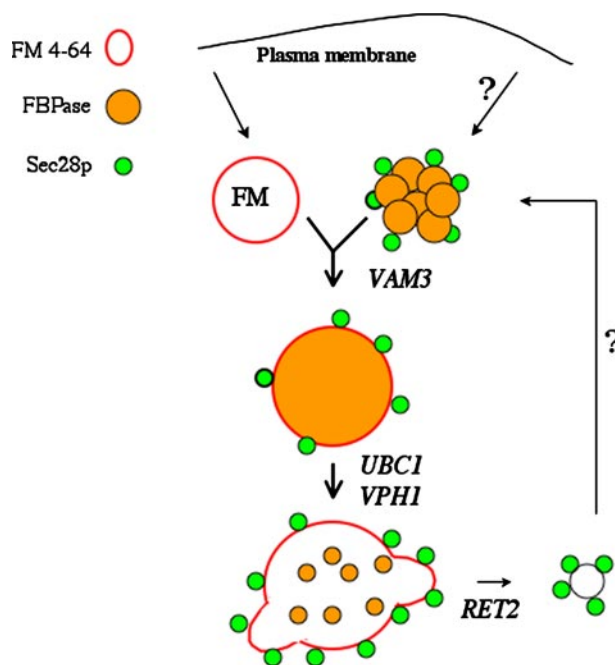


FIGURE 10. A model for the Sec28p trafficking pathway. Sec28p localizes on Vid vesicles and these vesicles converge with the endocytic pathway following a shift of cells to glucose. This process is regulated by the *VAM3* gene, and as such, Sec28p remains on Vid vesicles in cells lacking this gene. Following the fusion of endosomes with the vacuole, Sec28p is distributed on the vacuole membrane and then concentrates in vesicles that pinch off from the vacuole membrane. The *UBC1* gene most likely controls the concentration of Sec28p on the vacuole membrane, whereas *RET2* controls vesicle budding from the vacuole membrane. FBPase ultimately traffics to the vacuole, where it is degraded. Vid vesicles may be derived from the vacuole membrane. Alternatively, they may come from the plasma membrane, either directly or indirectly. The Sec28p anterograde trafficking pathway is utilized by cargo proteins such as FBPase. In $\Delta vph1$ cells, FBPase was detected within endocytic compartments. As with the Sec28p anterograde trafficking pathway, the *VAM3* gene plays an important role in the convergence of the FBPase trafficking pathway with the endocytic pathway.

punctate structures after a glucose shift. This mutant localized FM to small vesicles first and then large circular structures. FBPase was found in the lumen of these large structures after a longer shift to glucose. Thus, this suggests that FBPase enters the endocytic pathway as a luminal protein. This convergence is also likely controlled by the *VAM3* gene, because FBPase remained in Vid vesicles and did not co-localize with endocytic compartments, in cells lacking *VAM3*. These results further support our Sec28p results linking the Vid pathway with the endocytic pathway. Future experiments will be needed to address questions as to whether: 1) Vid vesicles are derived directly from the vacuole, 2) Vid vesicles are derived from the vacuole, traffic to the plasma membrane, and then pinch off from there, or 3) Vid vesicles are derived directly from the plasma membrane.

Acknowledgments—We thank Dr. R. Duden (University of Cambridge, UK) for generous gifts of the coatomer mutants *ret1-1*, *ret1-3*, *sec21-1*, *sec27-1*, and *anti-Sec28p* sera. We also thank Dr. Howard Riezman (University of Geneva, Switzerland) for the coatomer mutants *ret2-1*, *ret3-1*, *sec21-1*, and *sec27-1*. Anti-coatomer sera was from Dr. R. Schekman. MALDI analysis was performed by Dr. B. Stanley at the Core Facility of the Penn State College of Medicine. Primers used in this study were synthesized in the Core Facility at Penn State University College of Medicine.

REFERENCES

- Owen, D. J., Collins, B. M., and Evans, P. R. (2004) *Annu. Rev. Cell Dev. Biol.* **20**, 153–191
- Owen, D. J. (2004) *Biochem. Soc. Trans.* **32**, 1–14
- Wieland, F., and Harter, C. (1999) *Curr. Opin. Cell Biol.* **11**, 440–446
- Lee, M. C., Miller, E. A., Goldberg, J., Orci, L., and Schekman, R. (2004) *Annu. Rev. Cell Dev. Biol.* **20**, 87–123
- Bednarek, S. Y., Orci, L., and Schekman, R. (1996) *Trends Cell Biol.* **6**, 468–473
- Waters, M. G., Serafini, T., and Rothman, J. E. (1991) *Nature* **349**, 248–251
- Duden, R. (2003) *Mol. Membr. Biol.* **20**, 197–207
- Barlowe, C. (2003) *Trends Cell Biol.* **13**, 295–300
- Haucke, V. (2003) *Trends Cell Biol.* **13**, 59–60
- Palmer, K. J., and Stephens, D. J. (2004) *Trends Cell Biol.* **14**, 57–61
- Faulstich, D., Auerbach, S., Orci, L., Ravazzola, M., Wegchinger, S., Lottspeich, F., Stenbeck, G., Harter, C., Wieland, F. T., and Tschochner, H. (1996) *J. Cell Biol.* **135**, 53–61
- Eugster, A., Frigerio, G., Dale, M., and Duden, R. (2004) *Mol. Biol. Cell* **15**, 1011–1023
- Hosobuchi, M., Kreis, T. E., and Schekman, R. (1992) *Nature*. **360**, 603–605
- Duden, R., Griffiths, G., Frank, R., Argos, P., and Kreis, T. E. (1991) *Cell* **64**, 649–665
- Orci, L., Perrelet, A., Ravazzola, M., Amherdt, M., Rothman, J. E., and Schekman, R. (1994) *Proc. Natl. Acad. Sci. U. S. A.* **91**, 11924–11928
- Whitney, J. A., Gomez, M., Sheff, D., Kreis, T. E., and Mellman, I. (1995) *Cell* **83**, 703–713
- Aniento, F., Gu, F., Parton, R. G., and Gruenberg, J. (1996) *J. Cell Biol.* **133**, 29–41
- Gu, F., Aniento, F., Parton, R. G., and Gruenberg, J. (1997) *J. Cell Biol.* **139**, 1183–1195
- Piguet, V., Gu, F., Foti, M., Demaurex, N., Gruenberg, J., Carpentier, J. L., and Trono, D. (1999) *Cell* **97**, 63–73
- Daro, E., Sheff, D., Gomez, M., Kreis, T., and Mellman, I. (1997) *J. Cell Biol.* **139**, 1747–1759
- Gabrieli, G., Kama, R., and Gerst, J. (2007) *Mol. Cell. Biol.* **27**, 526–540
- Serafini, T., Orci, L., Amherdt, M., Brunner, M., Kahn, R. A., and Rothman, J. E. (1991) *Cell* **67**, 239–253
- Yorimitsu, T., and Klionsky, D. J. (2005) *Cell Death Differ.* **12**, 1542–1552
- Kamada, Y., Sekito, T., and Ohsumi, Y. (2004) *Curr. Top. Microbiol. Immunol.* **279**, 73–84
- Bowers, K., and Stevens, T. H. (2005) *Biochim. Biophys. Acta.* **1744**, 438–454
- Hurley, J. H., and Emr, S. D. (2006) *Annu. Rev. Biophys. Biomol. Struct.* **35**, 277–298
- Chiang, H.-L., and Schekman, R. (1991) *Nature* **350**, 313–318
- Chiang, M. C., and Chiang, H.-L. (1998) *J. Cell Biol.* **140**, 1347–1356
- Shieh, H.-L., and Chiang, H.-L. (1998) *J. Biol. Chem.* **273**, 3381–3387
- Hoffman, M., and Chiang, H.-L. (1996) *Genetics* **143**, 1555–1566
- Schork, S. M., Bee, G., Thumm, M., and Wolf, D. H. (1994) *FEBS Lett.* **349**, 270–274
- Hammerle, M., Bauer, J., Rose, M., Szallies, A., Thumm, M., Dusterhus, S., Mecke, D., Entian, K. D., and Wolf, D. H. (1998) *J. Biol. Chem.* **273**, 25000–25005
- Regelmann, J., Schule, T., Josupeit, F. S., Horak, J., Rose, M., Entian, K. D., Thumm, M., and Wolf, D. H. (2003) *Mol. Biol. Cell* **14**, 1652–1663
- Shieh, H. L., Chen, Y., Brown, C. R., and Chiang, H. L. (2001) *J. Biol. Chem.* **276**, 10398–10406
- Hung, G. C., Brown, C. R., Wolfe, A. B., Liu, J., and Chiang, H. L. (2004) *J. Biol. Chem.* **279**, 49138–49150
- Huang, P. H., and Chiang, H.-L. (1997) *J. Cell Biol.* **136**, 803–810
- Brown, C. R., McCann, J. A., and Chiang, H.-L. (2000) *J. Cell Biol.* **150**, 65–76
- Brown, C. R., McCann, J. A., Hung, G., Elco, C., and Chiang, H.-L. (2002) *J. Cell Sci.* **115**, 655–666

The Vid Degradation Pathway Merges with the Endocytic Pathway

39. Brown, C. R., Cui, D., Hung, G., and Chiang, H.-L. (2001) *J. Biol. Chem.* **276**, 48017–48026
40. Brown, C. R., Liu, J., Hung, G., Carter, D., Cui, D., and Chiang, H.-L. (2003) *J. Biol. Chem.* **278**, 25688–25699
41. Liu, J., Brown, C. R., and Chiang, H. L. (2005) *Autophagy* **1**, 146–156
42. Duden, R., Kajikawa, L., Wuestehube, L., and Schekman, R. (1998) *EMBO J.* **17**, 985–995
43. Kimata, Y., Higashio, H., Nies, A. T., Spring, H., Brom, M., and Keppler, D. (2000) *J. Biol. Chem.* **275**, 10655–10660
44. Bowser, R., Müller, H., Govindan, B., and Novick, P. (1992) *J. Cell Biol.* **118**, 1041–1056
45. Longtine, M. S., McKenzie, A., Demarini, D. J., Shah, N. G., Wach, A., Brachat, A., Philippsen, P., and Pringle, J. R. (1998) *Yeast* **14**, 953–961
46. Gaynor, E. C., Chen, C. Y., Emr, S. D., and Graham, T. R. (1998) *Mol. Biol. Cell* **9**, 653–670
47. Yahara, N., Ueda, T., Sato, K., and Nakano, A. (2001) *Mol. Biol. Cell* **12**, 221–238
48. Vida, T. A., and Emr, S. D. (1995) *J. Cell Biol.* **128**, 779–792
49. Raymond, C. K., Howald-Stevenson, I., Vater, C. A., and Stevens, T. H. (1992) *Mol. Biol. Cell* **3**, 1389–1402
50. Seeley, E. S., Kato, M., Margolis, N., Wickner, W., and Eitzen, G. (2002) *Mol. Biol. Cell* **13**, 782–794